Mechanistic Studies of Dichloro(1,4,7-triazacyclononane)copper(II)-Catalyzed Phosphate Diester Hydrolysis[†]

Kim A. Deal[‡] and Judith N. Burstyn*

Department of Chemistry, University of Wisconsin, 1101 University Avenue,
Madison, Wisconsin 53706

Received November 20, 1995[⊗]

In order to explore the role of labile metal complexes in promoting phosphodiester hydrolysis, detailed kinetic and mechanistic studies with Cu[9]aneN_3Cl_2 (**1**) were performed. The hydrolysis of bis(4-nitrophenyl) phosphate (**2**) by **1** is catalytic, as determined by the observation of both rate enhancement and turnover. The catalyst is selective for phosphodiesters; the rate of hydrolysis for 4-nitrophenyl phosphate (**4**) is 50 times slower than the hydrolysis rate of **2**. A rate enhancement of 2000 is observed relative to hydroxide ion mediated hydrolysis, and the rates reported herein are comparable to the rates reported for phosphodiester hydrolysis by other labile metal complexes. The reaction of **1** with **2** showed a half-order dependence on the catalyst, implicating a monomer−dimer equilibrium with the monomer as the catalyst. The kinetically determined equilibrium constant is 1220 M^{-1}, favoring the dimer. The reaction of **1** with ethyl 4-nitrophenyl phosphate (**3**) follows Michaelis−Menten kinetics ($K_M = 62.3$ mM and $k_{cat} = 1.96 \times 10^{-5}$ s^{-1}), providing evidence for the formation of a catalyst−substrate complex. The pH vs rate profile indicates that deprotonation of the metal-coordinated water ($pK_1 = 7.3$) occurs to form the active catalyst, and the reaction becomes pH independent above pH 8.5. The activation parameters for **3** hydrolysis by **1** (pH 9.0) are $\Delta H^{\ddagger} = 90$ kJ mol^{-1} and $\Delta S^{\ddagger} = -128$ J mol^{-1} K^{-1}. A mechanism consistent with the kinetic data is presented.

Phosphodiesters are exceptionally stable, making them uniquely suited to their role as the backbone for genetic material. Typical nucleases accelerate the rate of DNA hydrolysis by factors exceeding 10^{10}.[1] Most nucleases utilize metal ions as cofactors, but the precise role of the metal in the hydrolytic mechanism is unclear. In order to identify possible mechanisms by which metal ions promote phosphodiester hydrolysis, model compounds have been used to study the reactivity of coordinated phosphodiesters.[2] Hendry and Sargeson[3,4] have prepared exchange-inert amine complexes of Co(III) and Ir(III) containing a coordinated phosphodiester and a coordinated nucleophile. When a coordinated water molecule or ammine is deprotonated, the resulting hydroxide or amido ligand attacks the bound phosphodiester. In the case of Co(III), attack of a deprotonated ammine ligand on the coordinated phosphate ester results in the release of the activated leaving group and formation of a phosphoramidate ester chelate. The identification of this chelate species as the initial metal complex product verifies that the reaction proceeds via intramolecular nucleophilic attack.[3]

Labile and pseudolabile metal complexes have also been studied as potential hydrolysis catalysts, and the reactivities of these complexes support a mechanism in which a metal hydroxide serves as a nucleophile. Chin and co-workers[5] have studied a series of pseudolabile *cis*-$Co^{II}N_4(H_2O)_2^{3+}$ complexes, where N_4 is one of a number of facially chelating tetraamine ligands. Hydrolysis of the simple activated phosphodiester bis(4-nitrophenyl) phosphate in the presence of the cobalt complexes resulted in a reported dramatic increase in the observed first-order rate constant for the reaction. The pH dependence of the rate of reaction was consistent with the participation of a metal hydroxide in the hydrolysis.

Facile hydrolysis of phosphodiesters has been observed in the presence of labile metal complexes. Catalysis was observed with $Cu(bipy)^{2+}$: up to 1000 turnovers with a 10^3 rate enhancement at pH 8.5, when compared to a control reaction.[6] The rate of hydrolysis by $Cu(bipy)^{2+}$ increased dramatically with pH, consistent with the participation of a Cu−OH species in the hydrolytic mechanism. Evidence that the substrate phosphodiester was bound directly to the metal ion in the transition state was provided by the observation of saturation kinetics. Other labile metal complexes are effective, including those of zinc and nickel.[7,8] The complexes Zn[12]aneN_3^{2+} and Zn[12]aneN_4^{2+} effectively promoted the hydrolysis of phosphodiesters, and the pH dependence of the reactions was consistent with a metal hydroxide mechanism.[9] Interestingly, the tridentate complex Zn[12]aneN_3^{2+} was substantially more effective. This observation correlates with the lower pK_a for the coordinated water in Zn[12]aneN_3^{2+} and with the greater Lewis acidity of the zinc in a complex with fewer nitrogen donors.

The key role of the metal in promoting hydrolysis appears to be the intramolecular delivery of the nucleophile. By virtue of its Lewis acidity, the metal ion reduces the pK_a of a coordinated water molecule, thereby producing a good nucleophile at neutral pH. In addition, the hydration sphere normally

---

* Author to whom correspondence should be addressed.

[†] A portion of this work was published in preliminary form: Burstyn, J. N., Deal, K. A. *Inorg. Chem.* **1993**, *32*, 3585−3586.

[‡] In partial fulfillment of the Ph.D. degree in Chemistry; Ph.D. dissertation, Dec 1993.

[⊗] Abstract published in *Advance ACS Abstracts,* March 15, 1996.

(1) Serpersu, E. H.; Shortle, D.; Mildvan, A. S. *Biochemistry* **1987**, *26*, 1289−1300.
(2) Hendry, P.; Sargeson, A. M. In *Progress in Inorganic Chemistry*, Vol. 38; Lippard, S. J., Ed.; John Wiley & Sons: New York, 1990; pp 201−258.
(3) Hendry, P.; Sargeson, A. M. *Inorg. Chem.* **1990**, *29*, 92−97.
(4) Hendry, P.; Sargeson, A. M. *J. Am. Chem. Soc.* **1989**, *111*, 2521−2527.
(5) Chin, J.; Banaszczyk, M.; Jubian, V.; Zou, X. *J. Am. Chem. Soc.* **1989**, *111*, 186−190.
(6) Morrow, J. R.; Trogler, W. C. *Inorg. Chem.* **1988**, *27*, 3387−3394.
(7) Hikichi, S.; Tanaka, M.; Moro-oka, Y.; Kitajima, N. *J. Chem. Soc., Chem. Commun.* **1992**, 814−815.
(8) DeRosch, M. A.; Trogler, W. C. *Inorg. Chem.* **1990**, *29*, 2409−2416.
(9) Koike, T.; Kimura, E. *J. Am. Chem. Soc.* **1991**, *113*, 8935−8941.

S0020-1669(95)01488-1 CCC: $12.00

associated with a water molecule in bulk solution does not interfere with nucleophilic attack in an inner sphere reaction. Two important conclusions can be drawn from these studies that bear on the design of potential hydrolysis catalysts: (1) the metal ion must have two cis-oriented labile coordination sites in order to bind both the phosphodiester substrate and a water molecule in an orientation appropriate for intramolecular attack; (2) the metal must be a strong Lewis acid in order to facilitate deprotonation of the coordinated water to generate the hydroxide nucleophile.

As part of an ongoing effort to understand the mechanism of metal-promoted phosphodiester hydrolysis, we have examined in detail the mechanism by which Cu[9]aneN$_3$Cl$_2$ (**1**) facilitates the hydrolysis of activated phosphodiesters. We previously reported selective and catalytic hydrolysis of bis(4-nitrophenyl) phosphate to produce 4-nitrophenolate and 4-nitrophenyl phosphate (**4**).[10] Recently, we discovered that **1** is an effective catalyst for the hydrolysis of unactivated amides, including proteins.[11] This paper presents further kinetic studies of **1** mediated hydrolysis of **2** and ethyl 4-nitrophenyl phosphate (**3**). The hydrolytic efficiency of **1** is compared to that of the aforementioned metal complexes, and a mechanism for hydrolysis of phosphodiesters consistent with the kinetic data is presented.

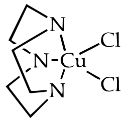

1

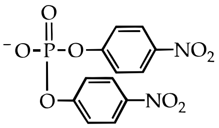

2

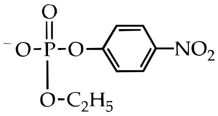

3

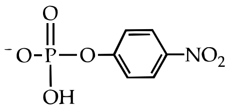

4

Experimental Methods

Materials. Sodium bis(4-nitrophenyl) phosphate, tetrasodium pyrophosphate, and the buffers HEPES (*N*-(2-hydroxyethyl)piperazine-*N*′-ethanesulfonic acid), MES (*N*-morpholineethanesulfonic acid potassium salt), EPPS (*N*-(2-hydroxyethyl)piperazine-*N*′-propanesulfonic acid), and CHES (2-(-cyclohexylamino)ethanesulfonic acid) were purchased from Sigma Chemical Co. Disodium 4-nitrophenyl phosphate was purchased from Pfaltz & Bauer, and 4-hydroxybenzaldehyde was purchased from Aldrich. Copper chloride was purchased from MCB, and all other chemicals used for synthesis were purchased from Aldrich. All chemicals were used without further purification. Aqueous solutions were prepared with water purified by passage through a Millipore purification system.

Instrumentation. An Orion Research digital ion analyzer, Model 611, equipped with a Ross semi-micro temperature compensation electrode was used for all pH measurements. Kinetic measurements were made with the use of a Hitachi U-3210 UV/visible spectrophotometer equipped with a water-jacketed cell holder. The temperature was regulated by an external circulating water bath (Lauda MT). The internal temperature of the reaction mixture was measured with a digital thermometer equipped with a type K thermocouple. A Waters isocratic HPLC pump, Model 6000A, with a Rheodyne injector and UV detector, Model 440, was used for HPLC measurements. Elemental analysis was performed by Galbraith Laboratories.

Preparation of Dichloro(1,4,7-triazacyclononane)copper(II). The ligand 1,4,7-triazacyclononane ([9]aneN$_3$) was prepared by literature methods and isolated as the trihydrochloride salt.[12−14] The catalyst, Cu[9]aneN$_3$Cl$_2$ (**1**), was prepared as described previously[15] by the reaction of 1 equiv each of [9]aneN$_3$·3HCl and CuCl$_2$·2H$_2$O with 3 equiv of NaOH in aqueous solution. The literature preparation involved impractical purification by manual separation of **1** from NaCl; a new separation procedure was developed to selectively precipitate the NaCl with ethanol. The mixture of NaCl and blue plates of **1** were dissolved in a minimum volume of hot water. The NaCl was selectively precipitated by the dropwise addition of ethanol until a faint turbidity persisted in the mixture. The mixture was chilled, the NaCl removed by filtration, and **1** recovered by evaporation over steam. The resulting blue powder was recrystallized from water to yield blue plates of **1** (yield 70%). The single-crystal X-ray structure was consistent with that previously reported. Anal. Calcd for C$_6$H$_{15}$N$_3$CuCl$_2$: C, 27.33; H, 5.73; N, 15.94; Cl, 26.89. Found: C, 27.17; H, 5.96; N, 15.79; Cl, 27.25.

Preparation of Sodium Ethyl 4-Nitrophenyl Phosphate. The substrate ethyl 4-nitrophenyl phosphate (**3**) was prepared by the literature method[4] and purified by anion exchange chromatography as described by Hengge and Cleland.[16] The diester was converted to the sodium salt by passing through a 5-fold molar excess of Dowex 50W (8%, 100−200 mesh) cation exchange resin prepared in the sodium form by equilibration with sodium acetate at pH 5.5 followed by washing with water. The eluent was concentrated by rotary evaporation to approximately 50 mL and then lyophilized to yield pure sodium ethyl 4-nitrophenyl phosphate. ^{1}H NMR (200 MHz, D$_2$O): δ 8.02 (d, 2H), 7.11 (d, 2H), 3.83 (m, 2H), 1.08 (t, 3H). ^{31}P NMR (500 mHz, D$_2$O): δ −2.42 (t).

Product Analysis. A 3.00 mL solution 5.00 mM in **2**, 1.00 mM in **1**, and 50 mM in buffer (HEPES, pH 7.24) was heated at 50 °C in a sand bath. Aliquots were withdrawn daily and the contents analyzed by reverse-phase HPLC on a Econosphere C-18 column (Alltech, 150 mm, 5 μm) using a mobile phase containing 50% methanol/50% 50 mM phosphate buffer, pH 7.0. Detection was by UV absorbance at 254 nm.

Kinetics. The initial rate of production of 4-nitrophenolate was monitored spectrophotometrically at 400 nm. Reactions performed at pH <9 were corrected for the degree of ionization of the 4-nitrophenol at the reaction temperature.[17] Correction for the spontaneous hydrolysis of the phosphate diester substrate was accomplished by direct difference, observing the production of 4-nitrophenolate relative to a reference cell containing no metal complex. The concentration of 4-nitrophenolate produced was calculated from the extinction coefficient (18 700 L mol^{-1} cm^{-1}). The initial rate of reaction was obtained directly from the plot of 4-nitrophenolate concentration versus time, which was linear with $R > 0.995$. All experiments were run in duplicate or triplicate, and the reported data represent the average values calculated from the linear regression of each individual data set. Agreement between the calculated initial rates for replicate experiments was within 5%.

In a typical experiment, freshly prepared **1** stock (10 mM) in water was added to 50 mM buffer (HEPES, MES, EPPS, or CHES), and the solution was heated in a Teflon-sealed screw cap cuvette to the reaction temperature. A reference, identical in all respects except lacking **1**, was similarly prepared. Freshly prepared **2** stock (10 mM) in water was added to both reaction mixtures, and the mixtures were allowed to equilibrate for 5 min. The increase in absorbance at 400 nm was followed with time, and the reaction was monitored for less than 5% conversion of substrate to products. Reactions were typically followed for 90 min; no change in the sample volume occurred. The total reaction volume was 3.00 mL, and the ionic strength was adjusted with

---

(10) Burstyn, J. N.; Deal, K. A. *Inorg. Chem.* **1993**, *32*, 3585−3586.

(11) Hegg, E. L.; Burstyn, J. N. *J. Am. Chem. Soc.* **1995**, *117*, 7015−7016.

(12) Koyama, H.; Yoshino, T. *Bull. Chem. Soc. Jpn.* **1972**, *45*, 481−484.

(13) Richman, J. E.; Adkins, T. J. *J. Am. Chem. Soc.* **1974**, *96*, 2268−2270.

(14) Searle, G. E.; Geue, R. J. *Aust. J. Chem.* **1984**, *37*, 959−970.

(15) Schwindinger, W. F.; Fawcett, T. G.; Lalancette, R. A.; Potenza, J. A.; Schugar, H. J. *Inorg. Chem.* **1980**, *19*, 1379−1381.

(16) Hengge, A. C.; Cleland, W. W. *J. Am. Chem. Soc.* **1991**, *113*, 5835−5841.

(17) Martell, A. E.; Smith, R. M. *Critical Stability Constants*; Plenum Press: New York, 1977.

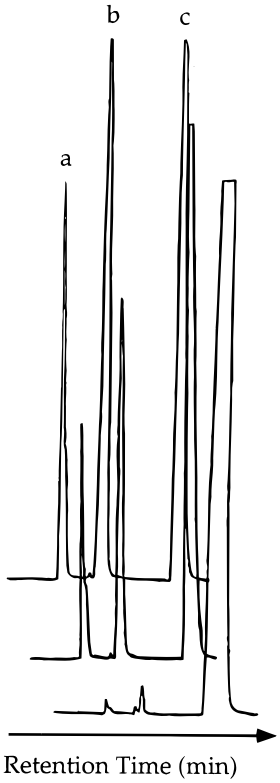

Figure 1. HPLC product separation of (a) 4-nitrophenyl phosphate at 1.4 min, (b) 4-nitrophenolate at 3.5 min, and (c) bis(4-nitrophenyl) phosphate at 4.3 min. Chromatographs were recorded after 1 h, 5 days, and 9 days. The mobile phase contained 1:1 methanol/50 mM phosphate buffer, pH 7.0.

5 M $NaClO_4$. First- and second-order rate constants were calculated from the initial rate on the basis of the determined reaction order with respect to **1** and the phosphate diester.

Activation parameters for the hydrolysis of **3** by the catalyst derived from **1** were calculated from the measured effect of temperature on the initial reaction rate. Four different temperatures were used from 30 to 90 °C; in one experiment the actual temperatures used were 29.5, 51.1, 69.5, and 88.2 °C. To ensure identical conditions of pH, concentration, and ionic strength, reaction mixtures were prepared in parallel and were pre-equilibrated at the desired temperatures. Reactions were performed in 50 mM CHES buffer, and the pH of the buffer was adjusted to 9.1 at each reaction temperature. Each reaction mixture contained 1.00 mM **1** and 10.0 mM **3** at an ionic strength of 0.1 M, controlled with 5 M $NaClO_4$. The measured temperatures are accurate to ±0.5 °C. To maintain a constant temperature at 32 °C, an external ice bath was used to cool the water circulator.

Results

Product Analysis. Products of the hydrolysis of **2** and **3** by **1** were identified by reverse-phase HPLC. In the hydrolysis of **2** by **1**, only **4** and 4-nitrophenolate were produced, and both products were detectable at short reaction times. The intensity of the two peaks grew at approximately the same rate over the entire reaction period of 10 days (Figure 1). The constant growth of the two product signals, combined with the linear decrease of the substrate peak, indicates that the phosphate monoester is hydrolyzed more slowly than the phosphate diester. Independent experiments using **4** as the substrate confirmed the slow rate of phosphate monoester hydrolysis. For the hydrolysis of **3** by **1**, only 4-nitrophenolate and unreacted substrate were detected by reverse-phase HPLC. The absence of 4-nitrophenyl phosphate indicated that the ethyl group was not hydrolyzed.

Kinetic Analysis. Kinetic studies of the hydrolysis of **2** and **3** by **1** were performed by applying the method of initial rates to determine the mechanism of metal mediated hydrolysis. Although only the first 5% of the reaction is observed, the method of initial rates is a convenient method for collecting kinetic data for slow reactions. The hydrolysis of **2** or **3** by **1** is a slow reaction, and it was not practical to follow the reaction for the minimum 3 half-lives required to directly measure the rate constant. Initially, control reactions were performed to check the accuracy of the assay and the stability of **1**. The hydrolysis of **2** by **1** was followed spectrophotometrically; the only significant spectral change occurred at 400 nm. The growth of the peak at 400 nm corresponded to the production of 4-nitrophenolate. No reaction was observed when [9]aneN_3 and $CuCl_2$ were added independently to **2**, and the $CuCl_2$ precipitated as copper hydroxide under the reaction conditions. The metal complex, **1**, was stable under the reaction conditions; no UV/visible spectral changes were noted when an aqueous solution of **1** was heated at 50 °C at pH 7.2 for 2 weeks.

Table 1. Kinetic Data for the Hydrolysis of Sodium Bis(4-nitrophenyl) Phosphate (**2**) by the Catalyst Derived from Cu[9]aneN_3Cl_2 (**1**) in Water at 50 °C as a Function of Metal Complex Concentration[a]

[Cu[9]aneN_3Cl_2] (mM)	initial rate[b] (10^{-10} M s^{-1})	[Cu[9]aneN_3Cl_2] (mM)	initial rate[b] (10^{-10} M s^{-1})
10.1	16.1	0.638	2.70
5.10	11.1	0.319	1.40
2.55	7.50	0.160	0.767
1.28	4.41		

[a] [**2**] = 0.100 mM; pH = 7.24 ± 0.02; 0.1 M HEPES; $\mu = 60 \pm 6$ mM; $T = 51.0 \pm 0.2$ °C. [b] Less than 5% conversion of substrate to products except for [**1**] = 10.1 mM (7.5%). Each reported rate is the average of three runs with less than 5% deviation among independently calculated rates.

Further experiments showed that the hydrolysis of **2** by **1** exhibited both a buffer effect and an ionic strength effect. The reaction rate decreased by nearly 15% for a 3-fold increase in the buffer concentration (0.1 to 0.3 M HEPES). The effect was sufficiently small that it was ignored in the kinetic analysis; constant buffer concentration was maintained through all subsequent experiments. A 100-fold increase in the ionic strength, adjusted with $NaClO_4$, resulted in a 30% decrease in the initial rate. The salt effect was significantly more pronounced when a salt containing a coordinating anion, such as chloride, was used. For detailed kinetic analysis, a constant ionic strength was used.

Phosphate diester hydrolysis catalyzed by **1** showed an unusual metal dependence which was explored in detail. The initial rate of hydrolysis of **2** by **1** shows a half-order dependence on the concentration of **1**, as shown in Table 1. This observation is consistent with the presence of a monomer−dimer equilibrium where the monomer is the hydrolysis catalyst. The concentration of the reactive monomer, LCu, can be calculated in terms of the total copper concentration, [Cu_T], by the mass balance relationship. Rearrangement results in a quadratic expression which gives the concentration of LCu in terms of [Cu_T]; the relationship between the square root of [Cu_T] and [LCu] is a parabola with an origin at 0,0. The experimental data will appear linear if K_f, the monomer−dimer equilibrium constant, times the concentration of **1** is greater than 0.25 ($2K_f[Cu_T] \gg 0.25$), and from the appropriate function (eq 1) the formation constant can be obtained.

$$[\mathrm{LCu}] = (-0.5 + (2K_f[\mathrm{Cu_T}])^{0.5})/2K_f \qquad (1)$$

In order to determine K_f from the kinetic data, it is necessary to relate the LCu concentration to the measured initial rate. The first step in the reaction mechanism must be binding of the active

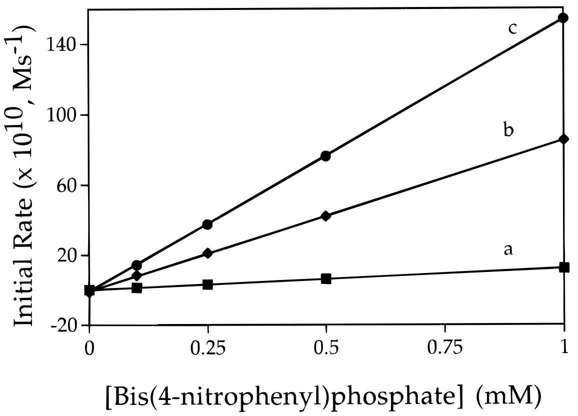

Figure 2. Dependence of the initial rate on the concentration of bis-(4-nitrophenyl) phosphate at (a) 0.3 mM, (b) 3 mM, and (c) 10 mM Cu[9]aneN$_3$Cl$_2$. pH = 7.24; T = 51.0 °C; μ = 60 mM. The plotted lines are least-squares fits to the data for which R > 0.995.

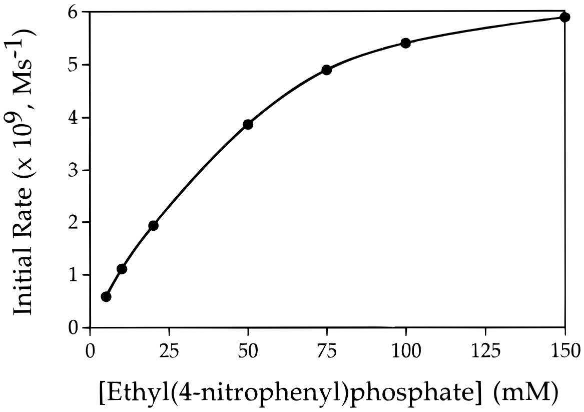

Figure 3. Saturation kinetics seen for the hydrolysis of sodium ethyl 4-nitrophenyl phosphate by the catalyst derived from Cu[9]aneN$_3$Cl$_2$. The data were fit to the Michaelis–Menten equation; the plotted line is the computer-generated best fit. K_M = 62.3 mM, V_{max} = 8.54 × 10^{-9} s^{-1}, and k_3 = 1.96 × 10^{-5} s^{-1}. pH = 7.24 ; T = 51.0 °C; μ = 0.5 M.

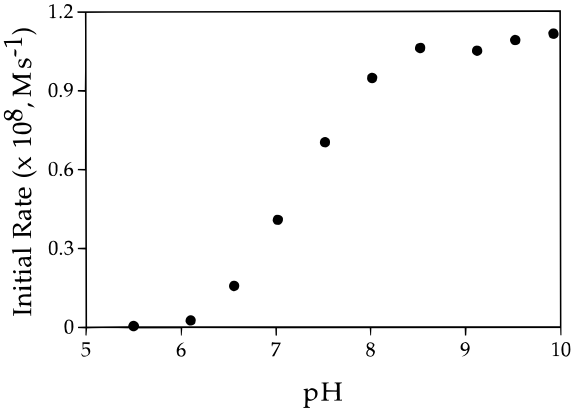

Figure 4. Dependence of the initial rate on pH for the hydrolysis of sodium bis(4-nitrophenyl) phosphate by the catalyst derived from Cu-[9]aneN$_3$Cl$_2$. [Cu[9]aneN$_3$Cl$_2$] = 1 mM; [bis(4-nitrophenyl) phosphate] = 0.1 mM; T = 51.0 °C; μ = 0.1 M; 50 mM HEPES, MES, CHES, or EPPS.

catalyst (LCu) to the phosphate diester $^-$OPO(OR)(OR′) which is described by K_2. In the second step, hydrolysis occurs and the products are released as described by k_3 . The rate equation (4) can be derived by assuming that the loss of product is the rate-limiting step ($k_3 \ll K_2$), providing the relationship needed between the concentration of CuL and the initial rate. Substitution of eq 1 into eq 4, followed by graphical analysis, will give the relationship between the initial rate and K_f. A dimer formation constant (K_f) of 1220 M^{-1} and an observed first-order rate constant ($k_{obs} = K_2k_3[^-OP(O)(OR)(OR')]$) of 8.86 × 10^{-7} s^{-1} are thus obtained.

$$\mathrm{LCu} + {}^-\mathrm{OPO(OR)(OR')} \overset{K_2}{\rightleftharpoons} \mathrm{LCu{-}OPO(OR)(OR')} \quad (2)$$

$$\mathrm{LCu{-}OPO(OR)(OR')} \xrightarrow{k_3} {}^-\mathrm{OR} + {}^{2-}\mathrm{OPO_2(OR')} \quad (3)$$

$$v = \mathrm{d[OR]}/\mathrm{d}t = K_2k_3[\mathrm{LCu}][{}^-\mathrm{OPO(OR)(OR')}] \quad (4)$$

The order of reaction with respect to substrate was determined for both **2** and **3**. Hydrolysis of these activated substrates by **1** is first order in substrate until extremely high concentrations of phosphate diester are reached relative to **1**. The hydrolysis of **2** by **1** is strictly first order in **2**, regardless of the concentration of **1** (Figure 2). Saturation was not attained, presumably due to the low affinity of **2** for **1**. Also, the limited solubility of **2** in water prevented more concentrated solutions of **2** from being prepared. When the more water-soluble phosphate diester **3** was used, saturation was observed. The hydrolysis of **3** by **1**, initially first order in **3**, became concentration independent at high ratios of **3** to **1**. The behavior can be fit to a modified Lineweaver–Burke function, where [LCu] is given in eq 1 and $K_M = (k_{-2} + k_3)/k_2$ (Figure 3). From this analysis, a Michaelis constant (K_M) of 62.3 mM, a maximal velocity (V_{max}) of 8.8 × 10^{-9} s^{-1}, and a first-order rate constant for the decomposition of the intermediate copper(II)–hydroxide–phosphate complex (k_3) of 1.96 × 10^{-5} s^{-1} were determined.

The effect of pH on the reaction rate was determined and correlated with the pK_a of a coordinated water in **1**. The pH versus rate profile shown in Figure 4 for the hydrolysis of **2** by **1** showed a pH-independent rate above pH 8.5 and a range below this pH where the initial rate of hydrolysis increases with pH. Independent potentiometric titration of **1** in 0.1 M NaClO$_4$ indicated that the deprotonation of the first coordinated water molecule occurred at pH 7.3. The pH profile, together with the potentiometric titration result, suggests that the large rate change is consistent with the deprotonation of a coordinated water to generate the catalytic species. The data can be fit to a rate expression for the hydrolysis of **2** by Cu[9]aneN$_3$(OH$_2$)-(OH)$^+$ where [LCu] is the total concentration of the active monomer defined in eq 1 and K_1 is the deprotonation equilibrium constant. Analysis of the data, by a nonlinear-least-squares fit of the plot of log (initial rate) versus pH, gave pK_1 = 7.3. The dip in the pH versus rate profile is consistent with a decrease in the rate of **1**-catalyzed hydrolysis upon deprotonation of the second water molecule coupled with a substantial increase in the hydroxide ion catalyzed hydrolysis at higher pH. The complete rate equation for the hydrolysis of **2** or **3** by **1** derived from the aforementioned considerations is given in eq 5.

$$v = \mathrm{d[OR]}/\mathrm{d}t = K_1K_2k_3[\mathrm{CuL}][{}^-\mathrm{OPO(OR)(OR')}]/([\mathrm{H}^+] + K_1) \quad (5)$$

Hydrolytic Efficiency. In order to compare the literature rate constants for metal-promoted phosphate diester hydrolysis with that measured in this study, it was necessary to adjust our data to match the varied published conditions. The initial rate of **1**-mediated hydrolysis of **2** was adjusted for temperature using the measured activation parameters within the temperature range used for the measurement of the activation parameters. The activation parameters for the hydrolysis of **2** by **1** were determined at pH 7.24 over the temperature range 30–90 °C.

Table 2. Comparison of the Rate Constants for Hydrolysis of Phosphate Diesters by Various Metal Complexes

nucleophile[a]	substrate	k(pH 7.2)[b]	T (°C)	ref
OH^-	**2**	$4 \times 10^{-7}\ s^{-1}$	100	18
$[9]Cu-OH^+$	**2**	$9 \times 10^{-4}\ s^{-1}$	100	
$(bpy)Cu-OH^+$	**3**	$1 \times 10^{-2}\ M^{-1}\ s^{-1}$	75	6
$[9]Cu-OH^+$	**2**	$5 \times 10^{-2}\ M^{-1}\ s^{-1}$	75	
$[12]Zn-OH^+$	**2**	$6 \times 10^{-5}\ M^{-1}\ s^{-1}$	35	9
$[9]Cu-OH^+$	**2**	$8 \times 10^{-4}\ M^{-1}\ s^{-1}$	35	
$(en)_2Co-OH^{2+}$	**2**	$3 \times 10^{-5}\ s^{-1}$	50	5
$[9]Cu-OH^+$	**2**	$9 \times 10^{-6}\ s^{-1}$	50	
$(en)_2Ir-OH^{2+}$	**3**	$3 \times 10^{-5}\ s^{-1}$	25	4
$[9]Cu-OH^+$	**2**	$5 \times 10^{-7}\ s^{-1}$	25	

[a] Abbreviations: bpy, 2,2′-bipyridine; [9], 1,4,7-triazacyclononane; [12], 1,5,9-triazacyclododecane; en, ethylenediamine. [b] The rate constants at pH 7.2 were derived from pH versus rate profiles in the listed references and are approximate.

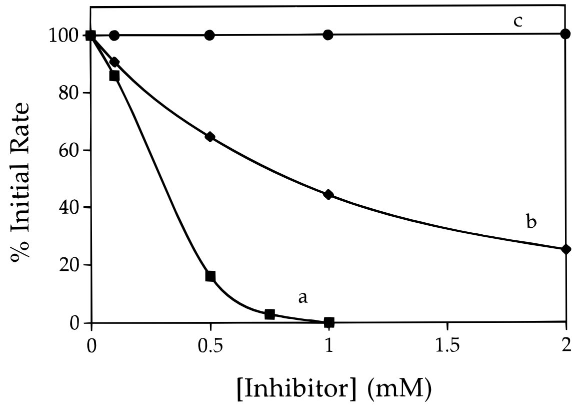

Figure 5. Percentage of initial rate retained in the presence of (a) pyrophosphate, (b) 4-nitrophenyl phosphate, and (c) 4-hydroxybenzaldehyde. [Cu[9]aneN$_3$Cl$_2$] = 1 mM; [bis(4-nitrophenyl) phosphate] = 3 mM; pH = 7.24 ; T = 51.0 °C; μ = 0.1 M. The computer-generated lines illustrate the trend in the data and have no mechanistic significance.

Data analysis was performed by use of the extended Arrhenius equation; a plot of ln(initial rate) versus 1/T was linear, yielding $\Delta H^\ddagger = 90 \pm 3$ kJ mol^{-1} and $\Delta S^\ddagger = -128 \pm 3$ J mol^{-1} K^{-1}. The error in the rate determinations within this temperature range was small, but extrapolation to conditions outside this range may not be accurate. Comparisons with published hydrolysis rates were limited to studies in which pH profiles were reported so that the rates of metal-promoted hydrolysis could be adjusted to pH 7.2. The measured initial rates for **1**-mediated hydrolysis were converted to calculated first-order rate constants by removing the **1** dependence according to eq 1. The second-order rate constant was calculated by dividing the calculated first-order rate constant by the substrate concentration. A summary of the calculated rate constants for **1** hydrolysis of **2** compared to the literature rate constants at pH 7.2 is given in Table 2.

Inhibition of Hydrolysis. Hydrolysis of phosphate diesters by **1** can be inhibited both by the product phosphate monoester and by chelating anions (Figure 5). Inhibition was observed for the hydrolysis of **2** by **1** on the addition of the phosphate monoester product **4**; 1 equiv of **4** relative to **1** quenched the initial rate of reaction to 48% of the uninhibited rate. The concentration dependence of inhibition by **4** did not fit a simple competitive inhibition model. Kinetic studies showed that **1** hydrolyzed **4** less rapidly than **2**, but both **2** and **4** give the same hydrolysis product, the 4-nitrophenolate ion measured in the assay, complicating analysis of inhibition of hydrolysis of **2** by **4**. The observed first-order rate constants for hydrolysis of **2**−**4** at pH 7.24 are listed in Table 3 for comparison.

Table 3. Observed First-Order Rate Constants for the Hydrolysis of Phosphate Esters by the Catalyst Derived from Cu[9]aneN$_3$Cl$_2$ (**1**)[a]

phosphate ester	k_{obs} (s^{-1})
$^{-}OPO(OC_2H_5)(OC_6H_4NO_2)$	7.2×10^{-8}
$^{-}OPO(OC_6H_4NO_2)_2$	1.3×10^{-6}
$^{2-}OPO(OC_6H_4NO_2)$	2.8×10^{-8}

[a] [**1**] = 1.00 mM; [phosphate ester] = 5.00 mM; pH = 7.24 ± 0.2; μ = 50 mM, T = 50 °C.

Inhibition by 4-nitrophenolate, the other product of the hydrolysis reaction, could not be tested directly because 4-nitrophenolate is the chromophore used in the spectrophotometric assay. Instead, 4-hydroxybenzaldehyde was used as a substitute for 4-nitrophenolate due to the similar pK_a's and the similar resonance stabilization of the two species. No inhibition was seen for 4-hydroxybenzaldehyde, even in the presence of 2 equiv of inhibitor relative to **1**.

Complete inhibition of hydrolysis of **2** by **1** was observed on the addition of the chelating anions pyrophosphate and oxalate. At one equivalent of pyrophosphate relative to **1**, no hydrolysis was observed. With 0.5 equiv of pyrophosphate relative to **1**, only 15% of the uninhibited rate was observed. Similar dramatic decreases in initial rate were observed for oxalate.

Discussion

Hydrolytic Efficiency. To evaluate the efficiency of **1**-catalyzed hydrolysis, the calculated first- and second-order rate constants were compared to relevant literature values (Table 2). Three sets of comparisons were made: first, **1** was compared to hydroxide ion, and it was found to be more efficient at comparable pH and concentration. Second, **1** was compared to substitutionally labile metal complexes and was found to be as efficient as Cu(bpy)$^{2+}$ and more efficient than Zn[12]aneN$_3$$^{2+}$. Finally, **1** was compared to substitutionally inert metal complexes and was found to be less efficient.

Phosphate diesters are extremely stable under most conditions (pH 2−10), and only highly activated phosphate diesters will hydrolyze at a reasonable rate at elevated temperature (100 °C) and pH (0.1 N NaOH).[18] Comparison of the catalytic rate constant for **1**-mediated hydrolysis relative to the rate constant for attack by hydroxide was carried out to assess the efficiency of **1** as a hydrolysis catalyst. From Table 2, the rate observed for **1**-mediated hydrolysis is 2000 times faster than the reaction with hydroxide; however, at pH 7.2, the concentration of OH$^-$ is low compared to the concentration of **1**, so a more valid comparison may be made at equivalent concentrations. The calculated rate constants for a reaction 0.3 mM in active catalyst derived from **1** (pH >8.5, k calculated from eq 4) or 0.1 mM in OH$^-$ [19] are 2×10^{-3} s^{-1} and 1×10^{-5} s^{-1}, respectively, yielding an approximate rate enhancement of 200 for **1**-mediated hydrolysis. This rate enhancement corresponds to a decrease in half-life from greater than 19 h for the hydroxide-catalyzed hydrolysis to less than 6 min for **1**-catalyzed hydrolysis; thus significant rate enhancements are observed when the rates of hydrolysis are compared both at a specific pH and at similar concentrations.

A second assessment of hydrolytic efficiency is obtained from the comparison of the rate constant for **1**-mediated hydrolysis relative to the rate constants for hydrolysis by other substitutionally labile metal complexes. Table 2 shows that the calculated rate constant for **1** is about equal to that of Cu(bpy)$^{2+}$ and larger

---

(18) Kirby, A. J.; Younas, M. *J. Chem. Soc. B* **1970**, 510−513.
(19) Kirby, A. J.; Younas, M. J. *J. Chem. Soc. B* **1970**, 1165−1172.

Scheme 1

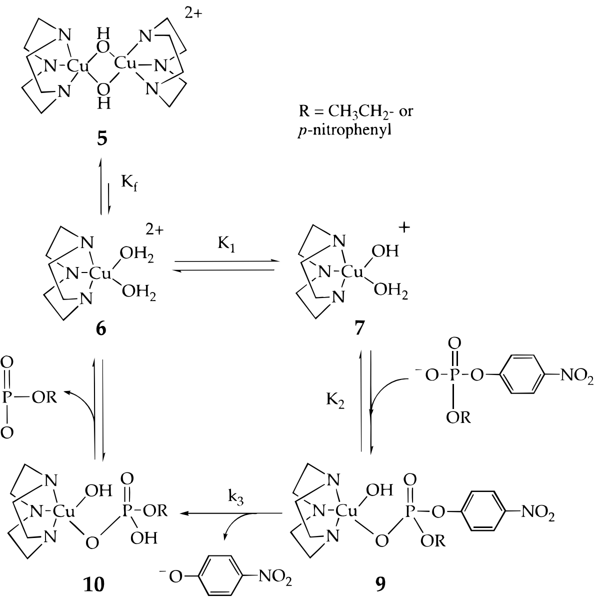

than that of $Zn[12]aneN_3^{2+}$. The slight rate enhancement observed with respect to $Cu(bpy)^{2+}$-mediated hydrolysis is not significant since there is a substantial reactivity difference between **2** and **3**, with **2** being the more reactive substrate. For $Cu(bpy)^{2+}$-mediated hydrolysis of **2** at pH 7.0, 1 mM $Cu(bpy)^{2+}$, and 50 °C, the rate constant is 3.5×10^{-6} s^{-1}, about twice the rate of **1** (2×10^{-6} s^{-1}) under the same conditions. The slightly larger rate constant is consistent with the more acidic pK_a of $Cu(bpy)^{2+}$ (7.0) relative to **1** (pK_a 7.3), providing further evidence that the Lewis acidity of the metal affects the rate of phosphate diester hydrolysis. Interestingly, the pK_a of $Zn[12]aneN_3^{2+}$ is the same as the pK_a of **1** (7.3), but **1**-promoted hydrolysis is 10 times faster. Since the relative Lewis acidities of the two species are equal, as measured by the pK_a of the coordinated water, other factors must affect the reactivity, including possibly the geometry of the metal complex and the donor strength of the ligands.

The final assessment of hydrolytic efficiency is obtained by comparing the rate of **1**-catalyzed hydrolysis to the rate of substitutionally inert metal complex promoted hydrolysis. As illustrated in Table 2, the calculated rate constant for **1**-catalyzed hydrolysis of **2** is slightly lower than that of $Co(en)_2^{3+}$ and substantially lower than that of $Ir(en)_2^{3+}$. The rate enhancement observed for $Co(en)_2^{3+}$ relative to **1** seems surprising since the ligand exchange rate of Cu(II) is $>10^9$ times faster than the ligand exchange rate of Co(III); however, Co(III) has a greater electrostatic attraction for the phosphate and is a harder Lewis acid than Cu(II) due to the increased charge-to-radius ratio for Co(III). The more effective charge neutralization and greater Lewis acidity of Co(III) could account for the observed rate enhancement. In the case of $Ir(en)_2^{3+}$-mediated hydrolysis, the metal complex is bound to the phosphate diester substrate through an oxygen ligand so that the hydroxide nucleophile on the iridium is aligned for intramolecular attack at the phosphorus center. The substrate–catalyst binding equilibrium is eliminated in this complex, and the resulting preorganization of catalyst and substrate is reflected in a significant rate enhancement compared to the case of **1**. The rate enhancement observed for $Ir(en)_2^{3+}$ is impressive considering the less reactive substrate **3** was used.

Mechanism of Phosphate Diester Hydrolysis. A mechanism proposed for **1**-catalyzed phosphate diester hydrolysis, consistent with the kinetic data, is shown in Scheme 1. When **1** is placed in aqueous solution, a dimer (**5**)–monomer (**6**) equilibrium is established where **6** is the precursor to the catalyst. The hydrolytically active species is obtained by deprotonation of a coordinated water with a pK_1 of 7.3 to form **7**. Species **7** is in rapid equilibrium with the catalyst–substrate complex, **9**, which is formed by the exchange of a coordinated water molecule for the phosphate diester substrate. Species **9** is hydrolyzed to 4-nitrophenolate and **10**. Species **10** dissociates to regenerate the precursor to the active catalyst and to release the phosphate monoester. Each step in this proposed mechanism will be discussed below.

The first step in the kinetic mechanism is the establishment of the copper dimer (**5**)–monomer (**6**) equilibrium. A bis(μ-hydroxo)-bridged copper(II) dimer of the 1,4,7-trimethyl derivative of [9]aneN$_3$ has been structurally characterized,[20] providing precedent for the formulation of the dimeric species in solution. Additional dimeric compounds of the form $[LCu(\mu\text{-}X)_2CuL]^{n+}$, where L = 1,4,7-$(CH_3)_3$-[9]aneN$_3$ and X = OH[21] or N$_3$,[22] have been characterized by X-ray structure analysis and by ESR spectroscopy. We have structurally characterized $[Cu_2([9]aneN_3)_2Cl_3]PF_6$ with a single μ-Cl bridge as well as the bis(μ-hydroxide)-bridged dimer $[Cu_2([10]aneN_3)_2(\mu\text{-}OH)_2]Br_2$,[23] demonstrating that dimeric copper(II) complexes of the nonalkylated [9]aneN$_3$ ligand are also stable.

In order for hydrolysis to occur, **5** must dissociate to **6**, as indicated by the half-order dependence of the rate of reaction on the concentration of **1**. Half-order dependence has been previously reported for several systems; for example, many reductions by dithionite ($S_2O_4^{2-}$) exhibit half-order dependence on $S_2O_4^{2-}$ due to the presence of $SO_2^{\bullet -}$.[24] In another case, Wilson and Cannon[25] observed a half-order dependence for the reduction of chromium(II) acetate, a reaction in which a dimeric species must dissociate into an active mononuclear chromium(II) species before reacting with a variety of oxidizing agents. For our system, a rapid equilibrium between **5** and **6** is likely, but **5** is the thermodynamically favored species as determined by the large K_f (1220 M^{-1}) favoring the dimer. Considering the low concentration of active complex in solution, relatively large rate enhancements for hydrolysis are observed.

It has been implied in the literature that a hydrolytically-active metal complex must have two substitutionally labile sites in a cis orientation, and one site must contain a potent nucleophile such as a coordinated hydroxide. The acidic form of the catalyst (**6**) does not contain a potent nucleophile and is largely unreactive, as demonstrated by the slow rate of hydrolysis below pH 7. Deprotonation of a coordinated water on **6** provides the necessary nucleophile; the kinetically determined equilibrium constant, pK_1 (7.3), correlates with the pK_a determined from the potentiometric titration of **1**. The agreement between K_1 and K_a provides strong evidence that the catalytically relevant proton is lost from a coordinated water molecule to generate the catalyst, **7**. Aquohydroxymetal complexes have previously been identified as the active species in other metal-promoted hydrolyses with both substitutionally inert and labile metal ions (vide supra). Given the pK_a of the coordinated water, it is clear that the active form of **1** will be available to carry out

---

(20) Chaudhuri, P.; Oder, K. *J. Chem. Soc., Dalton Trans.* **1990**, 1597–1605.

(21) Chaudhuri, P.; Oder, K.; Wieghardt, K.; Nuber, B.; Weiss, J. *Inorg. Chem.* **1986**, *25*, 2818–2824.

(22) Chaudhuri, P.; Ventur, D.; Wieghardt, K.; Peters, E. M.; Peters, K.; Simon, A. *Angew. Chem., Int. Ed. Engl.* **1985**, *24*, 57–59.

(23) Deal, K. A.; Cheung, C.-L.; Powell, D.; Burstyn, J. N. Unpublished results.

(24) Wilkins, R. G. *Kinetics and Mechanism of Reaction of Transition Metal Complexes*, 2nd ed.; VCH: Weinheim, Germany, 1991.

(25) Wilson, L. V.; Cannon, R. D. *Inorg. Chem.* **1985**, *24*, 4366–4371.

hydrolysis at physiological pH, an important requirement for hydrolysis of biologically relevant polymers. At very high pH, species **8** might be expected to form, resulting in a decrease in reaction rate due to loss of the active species. Experimentally, no such decrease in rate was noted up to pH 10, presumably due to the offsetting effect of the increasing rate of hydroxide-mediated hydrolysis.

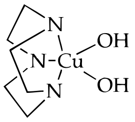

8

Evidence for the catalyst−substrate interaction was obtained by ^{31}P NMR and by the observation of saturation kinetics. The presence of a single, broad peak in the ^{31}P NMR spectrum for a sample of **1** with a molar excess of **3** indicates a fast exchange between **1** and **3**. Saturation kinetics with respect to **3** at high ratios of substrate to **1** provide further evidence for an intermediate copper(II) phosphate diester complex, **9**. Since ligand exchange in Cu(II) complexes is rapid compared to the rate of hydrolysis,[24] the rate-limiting step must involve the breakdown of **9** to products. Assuming the exchange of **3** as a ligand occurs much faster than hydrolysis ($k_{-2} \gg 2.0 \times 10^{-5}$ s^{-1} $= k_3$), then K_2 for coordination of **3** to **1** is approximately $1/K_M$, or 15 M^{-1}. A similar value of 20 M^{-1} has been reported for substrate-catalyst binding in Cu(bpy)$^{2+}$-catalyzed hydrolysis.[6] Phosphate diesters behave as weak ligands toward Cu(II),[17] and the small equilibrium constant measured in both of these systems presumably facilitates catalytic turnover on these complexes.

The inhibition observed for the hydrolysis of phosphate diesters by **1** by both the phosphate monoester product and chelating anions is consistent with the proposed mechanism. The product **4** is expected to bind to the copper ion with an affinity similar to that of **2**, and since both binding interactions are similarly reversible, competitive inhibition of the hydrolysis of **2** by **4**, is predicted. The inhibition observed did not fit a simple competitive model over a broad range of concentrations of **2** and **4**; however, at low concentrations of **2** relative to **4**, competition was observed. These observations are consistent with the formation of species **10**, which is proposed to dissociate to regenerate the catalyst. Hydrolysis of **2** by **1** was completely eliminated by both pyrophosphate and oxalate. As both inhibitors are bidentate chelating ligands, it is likely that dead-end copper chelate complexes are formed.

To ensure catalytic and selective hydrolysis, the active catalyst must be regenerated and the phosphate monoester released. Once hydrolysis occurs, the phosphate monoester is released from **10** and **6** is regenerated. As noted in Table 3, the hydrolysis of **4** is 50 times slower than the hydrolysis of **2**; this selective hydrolysis of the phosphate diester is unusual because the hydrolysis of phosphate monoester monoanions is generally much faster than that of diesters, and transition metal ions are known to promote both reactions.[2] The hydrolysis of **4** was accelerated in the presence of Co(III),[5] but Morrow and Trogler[6] saw a slight favoring of diester hydrolysis over monoester hydrolysis with Cu(bpy)$^{2+}$. That Co(III) and Cu(II) metal complexes respond differently to phosphate monoesters provides evidence that a mechanistic difference exists between the inert and labile metal complexes.

For hydrolysis to occur, the coordinated nucleophile must either directly attack the phosphorus center or activate a water molecule which will in turn attack the phosphorus center. In the mechanism described above, the formation of **9** preorganizes the coordinated hydroxide in an ideal position for intramolecular attack at the phosphorus. Rate accelerations of greater than 10^8 have been reported for intramolecular reactions, and the acceleration has been attributed to the template effect and other entropic contributions.[26] Intramolecular nucleophilic attack has been proposed to account for the large rate enhancements associated with cyclic phosphate diester hydrolysis[27] and ribonuclease action,[28] and in metal-promoted hydrolysis reactions, intramolecular attack of a transition metal coordinated hydroxide at a phosphate diester center has been elegantly demonstrated for phosphate monoesters and diesters.[4,29,30] In these studies, phosphate esters bound to substitutionally inert metal ions were employed, and intramolecular attack in these systems was proven by labeling studies. Since copper(II) readily exchanges aquo ligands on the hydrolysis time scale, no direct evidence for intramolecular or general-base intermolecular attack could be obtained by synthesizing labeled **1**.

It has been proposed that intramolecular attack of the metal-coordinated hydroxide will result in a five-coordinate phosphorane intermediate **11**. Alternatively, the reaction may proceed through a transition state characterized by simultaneous bond formation and bond cleavage. Indirect evidence for **11** has been obtained from labeling studies involving Co(III),[30] and a phosphorane intermediate has been invoked in the discussion of the mechanism for most substitutionally inert metal complexes.[4,5,31] A similar mechanism has been proposed for labile metal centers like Cu(II)[6,32] and Zn(II),[9,33] but there is no evidence for the phosphorane intermediate and recent studies of base-catalyzed hydrolysis of phosphate diesters with 4-nitrophenol leaving groups suggest that a concerted mechanism is operative.[16,34] Further investigations will be reported elsewhere providing evidence for a concerted transition state in labile metal systems.[35]

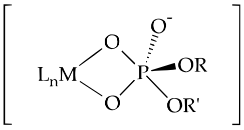

11

Acknowledgment. The authors thank W. W. Cleland, A. C. Hengge, and C. Landis for helpful discussions. K.A.D. acknowledges support from a Department of Education fellowship. Support of the Wisconsin Alumni Research Foundation is gratefully acknowledged.

Supporting Information Available: Tables and graphs of kinetic data and calculations of the adjustment of initial rates from the activation parameters (8 pages). This material is contained in many libraries on microfiche, immediately follows this article in the microfilm version of the journal, can be ordered from the ACS, and can be downloaded from the Internet; see any current masthead page for ordering information and Internet access instructions.

IC951488L

---

(26) Menger, F. M. *Acc. Chem. Res.* **1985**, *18*, 128−134.
(27) Westheimer, F. A. *Acc. Chem. Res.* **1968**, *1*, 70−78.
(28) Usher, D. A.; Richardson, D. I., Jr.; Oakenfull, D. G. *J. Am. Chem. Soc.* **1970**, *92*, 4699−4712.
(29) Harrowfield, J. M.; Jones, D. R.; Lindoy, L. F.; Sargeson, A. M. *J. Am. Chem. Soc.* **1980**, *102*, 7733−7741.
(30) Jones, D. R.; Lindoy, L. F.; Sargeson, A. M. *J. Am. Chem. Soc.* **1983**, *105*, 7327−7336.
(31) Kim, J. H.; Chin, J. *J. Am. Chem. Soc.* **1992**, *114*, 9792−9795.
(32) Menger, F. M.; Gan, L. H.; Johnson, E.; Durst, D. H. *J. Am. Chem. Soc.* **1987**, *109*, 2800−2803.
(33) Gellman, S. H.; Petter, R.; Breslow, R. *J. Am. Chem. Soc.* **1986**, *108*, 2388−2394.
(34) Hengge, A. C.; Cleland, W. W. *J. Am. Chem. Soc.* **1990**, *112*, 7421−7422.
(35) Deal, K. A.; Hengge, A. C.; Burstyn, J. N. *J. Am. Chem. Soc.* **1996**, *118*, 1713−1718.